

Chaotic biogeography algorithm for size and shape optimization of truss structures with frequency constraints

Shahin Jalili / Yousef Hosseinzadeh / Ali Kaveh

Received 2014-04-04, revised 2014-10-08, accepted 2014-10-09

Abstract

Size and shape optimization of truss structures with natural frequency constraints is inherently nonlinear dynamic optimization problem with several local optima. Therefore the optimization method should be sagacious enough to avoid being trapped in local optima and in this way to reduce premature convergence. To address this problem, we develop a Chaotic Biogeography-Based Optimization (CBBO) algorithm which combines the chaos theory and the biogeography-based optimization (BBO) to achieve an efficient optimization method. In this method, new chaotic migration and mutation operators are proposed to enhance the exploration ability of BBO. The performance of the method is demonstrated through five benchmark design examples with size and shape variables associated by multiply frequency constraints. The results show the efficiency and robustness of proposed method and in most cases, CBBO finds a relatively lighter structural weight than those previously reported results in the literature.

Keywords

Biogeography-based optimization · Chaos · Size and shape optimization · Truss structures

Shahin Jalili

Department of Civil Engineering, University of Tabriz, Building No. 7, 5166416471, Tabriz, Iran
e-mail: lshahin91@ms.tabrizu.ac.ir

Yousef Hosseinzadeh

Department of Civil Engineering, University of Tabriz, Building No. 7, 5166416471, Tabriz, Iran
e-mail: hosseinzadeh@tabrizu.ac.ir

Ali Kaveh

Center of Excellence for Fundamental Studies in Structural Engineering, University of Science and Technology, Narmak, Tehran-16, Iran
e-mail: alikaveh@iust.ac.ir

1 Introduction

With increasing the desire to minimize constructional costs of the structures and reducing the amount of material usage, optimal design of structures is gaining much attention. This paper addresses the optimal design of truss structures with natural frequency constraints, which has important applications in the dynamic response analyses.

In fact, in most of the low frequency vibration problems, the response of the structure to dynamic excitation is primarily a function of its fundamental frequency and mode shapes [1]. In some cases, a certain excitation frequency may cause resonance phenomenon. In such cases, the ability to manipulate the selected frequency can significantly improve the performance of the structure. Thus, the control of natural frequencies of the structure plays an important role to keep the structural behavior desirable.

Structural optimization with multiply frequency constraints is a highly nonlinear problem with respect to the design variables associated by non-convex solution space and multiple local minima which makes finding the global optimum a challenging problem. The main objective of this optimization is to minimize the weight of a structure, while satisfying the natural frequency constraints.

Over the past decades, many optimization algorithms have been developed for structural optimization problems with frequency constraints. The early works on the topics mostly use various classical techniques, such as Mathematical Programming (MP) and Optimality criteria (OC) methods, to size optimization of truss structures with frequency constraints. For example, Grandhi and Venkaya [2] used an optimality criterion method based on uniform Lagrangian density for resizing and a scaling procedure to locate the constraint boundary. Sedaghati et al. [3] employed the integrated force method to sizing both truss and beam structures under single and multiply frequency constraints.

On the other hand, the structure response is much more sensitive with respect to joint positions variation, and more effective designs can be generated by optimizing both shape and size parameters [4]. However, the complexity of the optimization

problem is increases by simultaneous consideration of size and shape variables. This complexity arises from different physical representation of these variables and, sometimes their changes are of widely different orders of magnitude. During the last two decades a number of researches have utilized classical optimization techniques. For instance, Wang et al. [5] proposed an optimality criteria algorithm for combined sizing-layout optimization of three-dimensional truss structure. In this method, the sensitivity analysis helps to determine the search direction and the optimal solution is achieved gradually from an infeasible starting point with a minimum weight increment, and the structural weight is indirectly minimized.

Generally, the above-mentioned classical optimization techniques have several drawbacks, such as computational complexity, dependence on good starting point and premature convergence. As an alternative to the classical optimization approaches, meta-heuristic optimization techniques have been widely utilized and improved to solve engineering optimization problems characterized by non-convex, dis-continuous and non-differentiable. Meta-heuristic algorithms, such as Genetic Algorithm [6], Particle Swarm Optimizer [7], Charged System Search [8] and Big Bang-Big Crunch [9] algorithm are developed by the simulation of the natural processes trying to solve complex optimization problems in a stochastic manner, where other optimization methods have failed to be effective.

Genetic Algorithm (GA) developed by Goldberg [6], inspired from human evolution principles, such as inheritance, mutation, selection, and crossover. Lingyun et al. [10] introduced hybrid Niche Hybrid Genetic Algorithm (NHGA) to shape and size optimization of truss structures with frequency constraints. In this method, the exploitation capacities of GA are enhanced while the diversity of population is maintained. In addition, the simplex search is used as a local search operator.

Particle Swarm Optimizer (PSO) originally developed by Kennedy and Eberhart [7] is inspired by social behavior of bird flocking or fish schooling. Gomes [11] utilized standard PSO to optimization of truss structures with dynamic constraints. Recently, Kaveh and Zolghadr [12] introduced democratic particle swarm optimization (DPSO) to mass minimization of trusses with frequency constraints. In this method, the exploration capability of standard PSO is improved by using the information produced by all of the eligible members of the swarm. As the name suggests, in the DPSO algorithm all of the better particles and some of the worse particles affect the new position of the particle under consideration.

Kaveh and Zolghadr [13] proposed a hybridized Charged System Search and Big Bang-Big Crunch algorithm (CSS-BBBC) with trap recognition capability for weight optimization of trusses on layout and size. This hybrid algorithm, improved the diversification properties of the standard CSS and uses BB-BC algorithm to maintain an extra disturbance and to help the agents to leave the trap. Charged System Search (CSS) algorithm developed by Kaveh and Talatahari [8] is one of the most

recent optimization algorithms. The method utilizes the governing Coulomb law from electrostatics and the Newtonian laws of mechanics to simulate the charged particles, which can affect each other based on their fitness values and their separation distances [8]. In addition, the Big Bang-Big Crunch (BB-BC) algorithm was developed by Erol and Eksin [9]. It is based on the theory of the evolution of the universe; namely, the Big Bang and Big Crunch theory. The BB-BC consists of two phase: Big-bang phase and Big-crunch phase. In the Big Bang phase, energy dissipation produces disorder and randomness is the main feature of this phase; whereas, in the Big Crunch phase, randomly distributed particles are drawn into an order [9].

Recently, a new population-based meta-heuristic algorithm based on the biogeography theory, namely Biogeography-Based Optimization (BBO), is introduced by Simon [14]. The biogeography theory, describes the geographical distribution of biological organisms. The framework of BBO inspired from mathematical models of biogeography which is developed by MacArthur and Wilson [15]. These mathematical models state that how species migrate between the islands (habitats) [14]. BBO is a successful heuristic search technique that has been successfully applied to global optimization of numerical functions [16, 17] and were used to solve numerous real-world optimization problems [14, 18, 19]. However, despite having a good exploitation ability, the standard BBO has the problem of premature convergence. The main reason of poor exploration ability of standard BBO arises from it is migration operator. In the consecutive generations, the poor solutions are probabilistically updated by the migration operator, which shares the information of good solutions. After several generations, the current solutions finally converge to the same local optimum and the migration operator shares similar information among solutions. Although this similar information sharing leads to good exploitation capability, but it considerably decreases the exploration ability of BBO. In addition, the simple stochastic mutation operator of BBO may lead to revisiting non-productive regions of the search space.

As a kind of characteristic of non-linear systems, chaos is a bounded unstable dynamic behavior that exhibits sensitive dependence on initial conditions and includes infinite unstable periodic motions [2]. Chaos is a deterministic process with stochastic appearance exhibited by a deterministic nonlinear system. Due to the non-repetition of chaos, it can carry out overall searches at higher speeds than stochastic ergodic searches that depend on probabilities [21]. Chaotic sequences are very sensitive to the initial conditions and two quite different sequences can be generated by the two very close initial parameters. Recently, many researchers have used the idea of employing chaotic sequences during the optimization process of meta-heuristics instead of random sequences, such as chaotic particle swarm optimization (CPSO) [22, 23], chaotic differential evolution (CDE) [24] and chaotic harmony search (CHS) [25]. The choice of chaotic sequences is justified theoretically by their unpredictability, i.e., by their spread-spectrum characteristic and

ergodic properties [25].

In the present study, the BBO is combined with the chaos theory to obtain a new optimization method called the Chaotic Biogeography-Based Optimization (CBBO) to size and shape optimization of truss structures with frequency constraints. In order to accelerate the convergence speed, two operators based on Chaos theory are developed, namely chaotic migration and mutation operators. The proposed migration operator employs logistic map function and a selection strategy for efficient information sharing between the habitats. Through this migration scheme, the exploration ability of the algorithm is increased and CBBO can quickly and accurately find an near-optimum solution. In addition, based on the ergodicity, symmetry and stochastic property of the improved logistic map function, we develop new mutation operator to increase the population diversity. A set of five well-known design examples are considered to validate the efficiency of the proposed method. The simulation results validate the superiority of the new method in obtaining optimal designs as compared with other methods.

The rest of the paper is organized as follows. Section 2 provides a mathematical description of the optimum design problem. In Section 3 the simple BBO and chaotic sequences are briefly described and then the proposed CBBO algorithm are presented and explained in detail. Five optimal design examples illustrating the efficiency of the proposed algorithm are covered in the Section 4. Finally, conclusions are presented in Section 5

2 Mathematical description of the optimum design problem

The main aim of layout and size optimization of a truss structure is to minimize the weight of the structure while satisfying some constraints on natural frequencies. In this class of optimization problems, cross-sectional areas and nodal coordinates are taken as design variables. The optimal design of a truss structure can be formulated as:

$$\begin{aligned} &\text{Find } X = [x_1, x_2, \dots, x_n] \\ &\text{To minimize } W(X) = \sum_{i=1}^m \rho_i A_i L_i \end{aligned} \quad (1)$$

Subjected to:

$$\begin{aligned} g(X) &= \frac{\omega_j}{\omega_j^*} - 1 \geq 0, \quad \text{for some natural frequencies } j \\ h(X) &= \frac{\omega_k}{\omega_k^*} - 1 \leq 0, \quad \text{for some natural frequencies } k \\ x_i^{\min} &\leq x_i \leq x_i^{\max}, \end{aligned}$$

Where X is the vector containing the design variables, including both nodal coordinates and cross-sectional areas; n is the number of design variables; $W(X)$ is the weight of the structure; m is the number of members making up the structure; ρ_i is the density of member i ; A_i is the cross-sectional area of the member i ; L_i is the length of the member i ; $g(X)$ and $h(X)$ are the constraint violations for natural frequencies of the structure; ω_j and

ω_j^* are the j th natural frequency of the structure and corresponding lower limit, respectively; ω_k is the k th natural frequency of the structure and ω_k^* is its upper bound; x_i^{\min} and x_i^{\max} are the lower and upper bounds of the i th design variable, respectively.

Optimal design of truss structure should satisfy the above mentioned constraints. In this study, the constraints are handled by using a simple penalty function method, which can guide the unfeasible candidate solutions to move to the feasible regions of search space. Thus we define the fitness function for each solution candidates. The fitness function of solution candidate X is defined as follow:

$$F_{fitness} = W(X) \times f_{penalty} \quad (2)$$

$$f_{penalty} = (1 + \varepsilon_1 \cdot \varphi)^{\varepsilon_2}, \quad \varphi = \sum_{i=1}^q \varphi_i \quad (3)$$

Where $f_{penalty}$, is the penalty function represented by individual X , q is the number of constraint violation and φ is the penalty factor which is related to the violation of constraints. In order to obtain the values of φ_i the natural frequencies of the structure are compared to the corresponding upper or lower bounds. For example for j th frequency constraint, the penalty factor is calculated as follow:

$$\begin{cases} \varphi_j = \left| \frac{\omega_j^* - \omega_j}{\omega_j^*} \right| & \text{for } \omega_j < \omega_j^* \\ \varphi_j = 0 & \text{for } \omega_j \geq \omega_j^* \end{cases} \quad (4)$$

As it can be seen from Eq. (2), if the constraints are not violated, the value of the penalty function will be zero. In Eq. (3), the parameters ε_1 and ε_2 are selected considering the exploration and the exploitation rate of the search space. In this study ε_1 is taken as unity and ε_2 starts from 2 and gradually increases. The value of ε_2 for t th iteration is calculated as follow:

$$\varepsilon_2^{(t)} = \varepsilon_2^{(t-1)} + 10^{-3} t \quad (5)$$

3 Optimization method

3.1 Biogeography-based optimization (BBO)

BBO is a simple and efficient optimization algorithm originally proposed and shown effective for finding global optima for some optimization problems by Simon [14]. In fact, BBO is a population-based meta-heuristic algorithm motivated by migration behavior of species between the habitats, in which each habitat is a solution candidate for the optimization problem. In BBO, the position of each habitat H in an n -dimensional search space is represented by suitability index variables (SIVs), which is an n -dimensional vector The fitness value of each habitat is demonstrated by Habitat Suitability Index (HSI).

Habitats with a high HSI tend to have a large number of species, while those with a low HSI have a small number of species [14]. The two main operators of this algorithm are *Migration* and *Mutation* operators

In the BBO approach, the emigration and immigration process is done by migration operator between good and poor habitats to share information about the appropriate habitats which are possible solutions for optimization problem. This information sharing depends on the immigration rate λ and emigration rate μ of each habitat, which are functions of the number of species in the habitat. These can be calculated by Eq. (6) and Eq. (7), as follows [14]:

$$\lambda_k = I \left(1 - \frac{K}{S_{max}} \right) \quad (6)$$

$$\mu_k = E \left(\frac{K}{S_{max}} \right) \quad (7)$$

Where I is the maximum possible immigration rate; E is the maximum possible emigration rate; K is the number of species of the k th habitat and S_{max} is the maximum number of species. Fig. 1 illustrates a linear migration model for the case of $E = I$. As it can be seen from Fig. 1, the habitat which has few species (poor solution, low HSI) like S_1 has a low emigration rate and a high immigration rate. This means that, the habitat with low HSI have a greater chance to take information about the good habitats. On the other hand, the habitat which has more species (good solution, high HSI) like S_2 has a low immigration rate and a high emigration rate. In this way, the habitat with high HSI tends to share its good information among the habitats. In addition, the habitat with medium HSI, like point S_0 , both immigration and emigration rates are equal, in which the probability of taking or giving information from or to other habitats is equal. The point S_0 is the equilibrium number of species. The migration operator can be described as follow:

$$H_i(SIV) \leftarrow H_j(SIV) \quad (8)$$

Where H_i and H_j are the immigrating and emigrating habitats, respectively. These habitats, is the probabilistically selected habitats based on the immigration and emigration rates. Fig. 2 depicts the migration producer of BBO algorithm.

After migration operator, BBO utilizes the mutation operator to increase the population diversity. The mutation operator is a probabilistic operator that modifies a habitat's SIV randomly based on mutation rate $pMutate$ that is related to the habitat probability. The mutation rate $pMutate$ is calculated as follows:

$$pMutate = m_{max} \left(\frac{1 - P_i}{P_{max}} \right) \quad (9)$$

Where m_{max} is a user-defined parameter and $P_{max} = \max\{P_i\}$. The complete details for the calculation of P_{max} and P_i can be found in [14]. According Eq. (9), each habitat has a different chance to mutate, but in this paper the same mutation probability are considered for all habitats. The mutation operator of BBO algorithm can be described as Fig. 3.

Another feature of BBO is that some habitats with high HSI (elites) selected by the parameter of *KeepRate* to keep elites

from one generation to the next. It means that, the new habitats of current iteration combined with some elites from prior iteration. After combining habitats, habitats with high HSI are selected to the formation of new population. In this study, the value of parameter *KeepRate* is set to 0.1 for all numerical examples. For example, when the number of habitats is 50, five habitats with high HSI are selected to keep.

3.2 Chaotic sequence

Chaos is a deterministic process with stochastic appearance exhibited by a deterministic nonlinear system in which small changes in the parameters or the starting values for the data lead to different future behaviors, such as stable fixed points, periodic oscillations, bifurcations, and ergodicity [26]. Recently, chaotic sequences are used in place of random sequences during the optimization process. There are various one-dimensional chaotic maps to generate chaotic sequences such as Logistic map, Kent map, Bernoulli shift map, Sine map and Circle map. Logistic map is one of the most used chaotic maps in literature. It has been brought to the attention of researchers by May [27] which often cited as an example of how complex behavior can arise from simple dynamic systems. The simple Logistic chaotic map is described as follows:

$$y_{t+1} = \beta y_t (1 - y_t), \quad t = 1, 2, \dots; \quad y_0 \in (0, 1) \quad (10)$$

Where β is the control parameter, y_t is a chaotic variable in iteration t . It can be mathematically prove that the system with initial condition $y_0 \notin (0, 0.25, 0.5, 0.75)$, is entirely in chaotic status when $\beta = 4$. Fig. 4 shows the ergodic property and the probability distribution of the Logistic map function considering the initial value of $y_0 = 0.35$ and 3000 iterations. By setting $y_t = (z_t + 1) / 2$ in Eq. (8), the improved chaotic logistic map with symmetrical region $(-1, 1)$ is expressed as Eq. (9) [28]:

$$z_{t+1} = 1 - 2z_t^2, \quad t = 1, 2, \dots; \quad z_t \in (-1, 1) \quad (11)$$

Fig. 5 shows the ergodic property and the probability distribution of the improved logistic map function considering the initial value of $z_0 = 0.35$ and 3000 iterations.

3.3 Chaotic biogeography-based optimization (CBBO)

As mentioned before, the basic BBO, which has been widely used to solve various scientific and engineering optimization problems, employs simple migration and mutation operators. However, such simple operators may lead to some disadvantages such as a low exploration ability and premature convergence. In Eq. (8), the immigrating habitat updated by simply replacing one of the SIV of emigrating habitat randomly, which often implies a rapid loss of diversity in the population. On the other hand, the purely random mutation operator of BBO may lead to revisiting non-productive regions of the search space which lead to long computing time. To cope with these disadvantages of BBO,

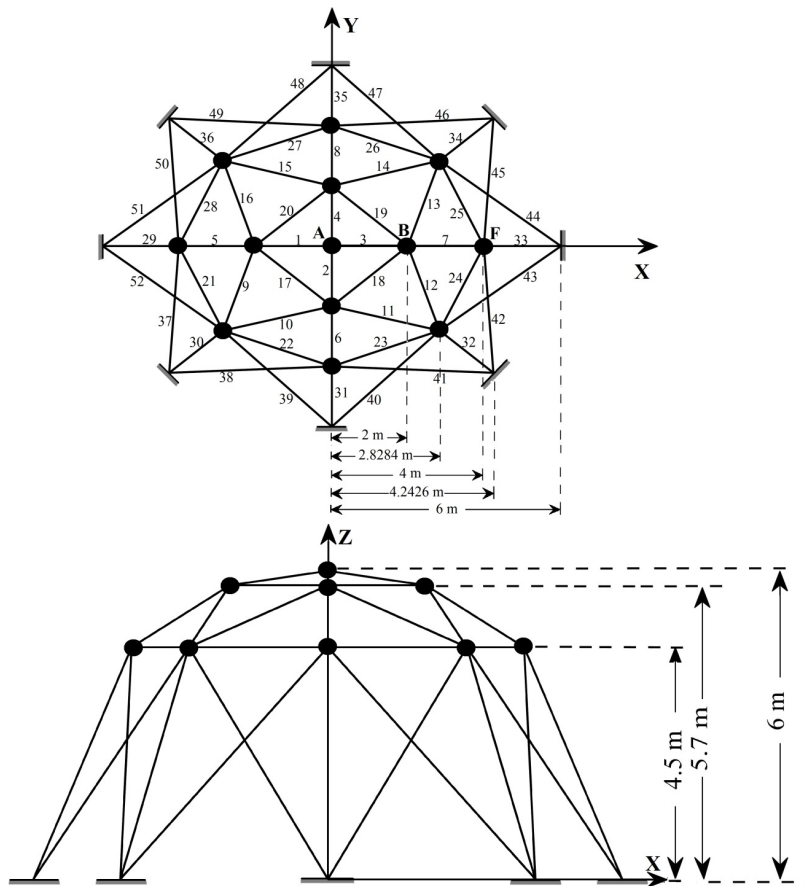


Fig. 1. The simple linear migration model. Emigration and immigration rates for case $E = I$.

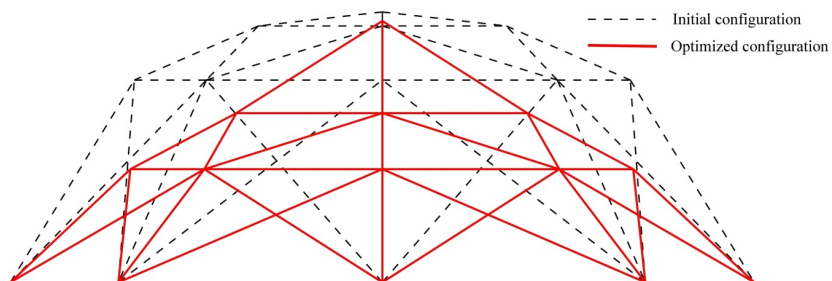


Fig. 2. The migration operator of BBO.

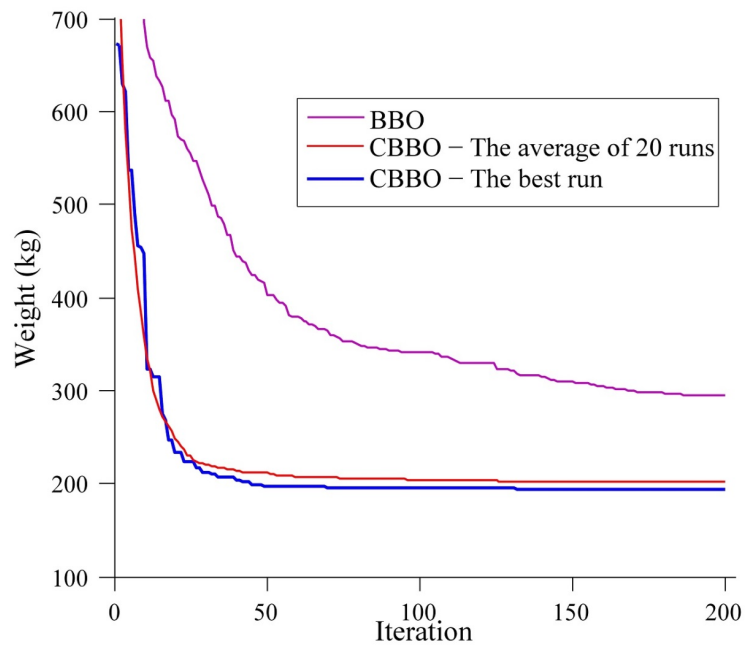


Fig. 3. The mutation operator of BBO.

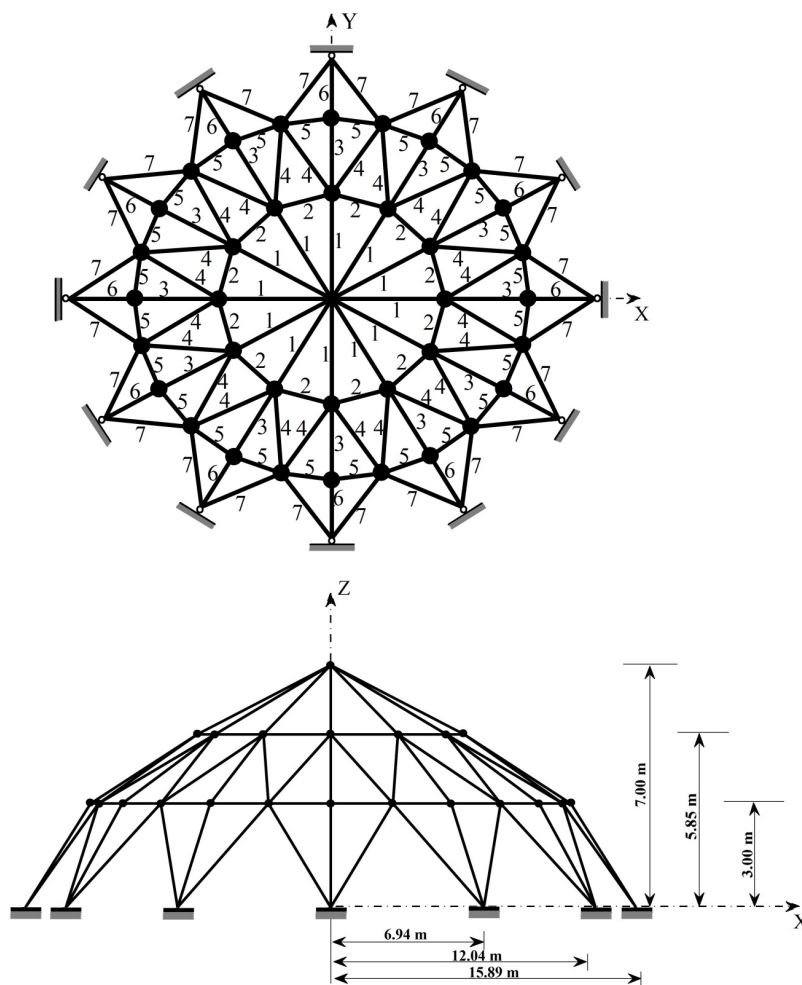


Fig. 4. The ergodic property and the probability distribution of the logistic map function with the initial value of $y_0 = 0.35$ and 3000 iterations.

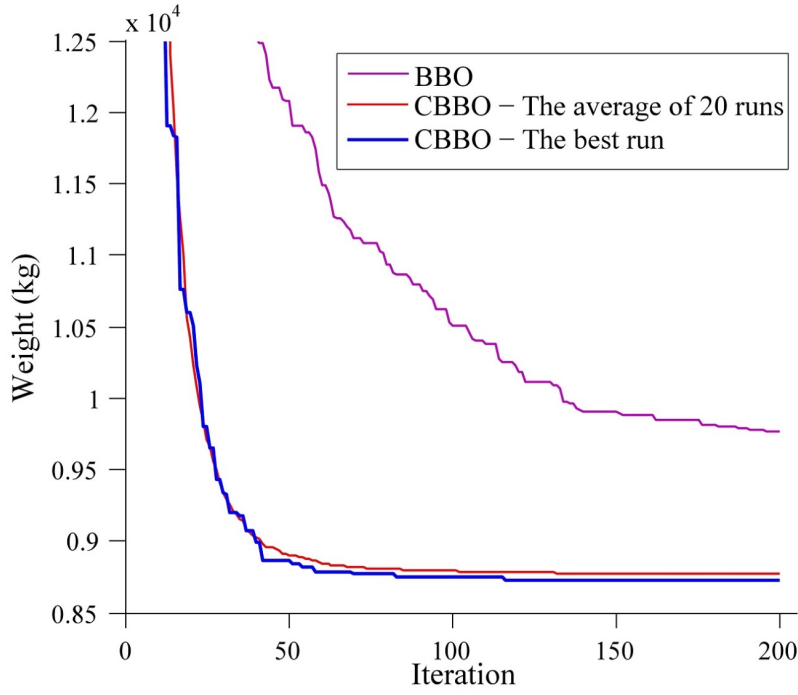


Fig. 5. The ergodic property and the probability distribution of the improved logistic map function with the initial value of $z_0 = 0.35$ and 3000 iterations.

A Chaotic Biogeography-Based optimization (CBBO) based on new chaotic migration and mutation operators is proposed

During the information sharing process of the migration operator, some habitats may be trapped into local optimum and it is necessary to exchange the solution space information among the whole population, efficiently. Thus, the migration operator should provide a variety of information about the population between the habitats. In order to get a better performance including the better solution and convergence speed, the new logistic map based migration operator is described as follows:

$$H_i(k) = H_i(k) + c_1 \times y_t^{(1)} \times (H_j(k) - H_i(k)) + c_2 \times y_t^{(2)} \times (H_l(k) - H_i(k)) \quad (12)$$

Where H_i is the immigrating habitat, H_j and H_l are the emigrating habitats, c_1 and c_2 are two positive constants which adjust the influence degree of two selected emigrating habitats and y_t is the chaotic variable between (0, 1) generated by Eq. (10). It is important to note that, $y_t^{(1)}$ and $y_t^{(2)}$ are two different chaotic sequences with different initial value (y_0) generated by Eq. (10). The initial values for chaotic sequences are randomly selected between 0 and 1, except points (0, 0.25, 0.5, 0.75). Here the two emigrating habitats H_j and H_l are selected probabilistically based on emigration rates. At each iteration cycle, the k th variable of position of habitats is updated by Eq. (12). Note that, whenever the updated position of a habitat goes beyond its lower or upper bound, the habitat will take the value of its corresponding lower or upper bound.

The proposed migration operator appears to be more useful because it takes into consideration two different habitats. As

mentioned before, the emigrating habitats are randomly selected based on their emigrating rates, and the emigration rates are directly proportional to the HSI values (fitness values). In fact, according to Eq. (12), all of the better and worse habitats affect the new position of the habitat under consideration, but the habitats with high HSI have a high chance to affect the new position. This migration scheme can improve the exploration ability of the algorithm and alleviate premature convergence.

After migration operator, each variable of a habitat is mutated according to the mutation probability ($pMutation$). As mentioned before, standard BBO uses a purely random generation to mutate habitats, which leads to revisiting non-productive regions of the search space and often exhibit unacceptably slow convergence rate. In order to reduce the effects of purely random mutation and to prevent the local trapping of the algorithm, the new improved logistic map based mutation operator for k th variable of i th habitat is described as follow:

$$H_i(k) = H_i(k) + z_t \times \alpha \times (H_{max}(k) - H_{min}(k)) \quad (13)$$

Where z_t is the chaotic variable between (-1, 1) generated by Eq. (11), α is the user defined parameter, $H_{max}(k)$ showing the upper bound and $H_{min}(k)$ indicating the lower bound for variable k .

It seems that the values of low mutation probabilities ($pMutation$) is appropriate values and high values of this parameter may not be suitable. This parameter is usually set as too small to get good results. In this study, the value of mutation probability ($pMutation$) is considered as 0.1 for all experiments.

The value of α controls search length of the mutation operator. A small length may be inefficient in exploring different regions

of the search space and therefore unsuccessful at improving the search quality. On the other hand, with a longer length, the mutation operator may cause revisiting non-productive regions unnecessarily.

In order to better explain the algorithm, the detailed steps of CBBO can be summarized as below:

Step 1: define the optimization problem, set the initial values for chaotic sequences (z_0 and y_0) and initialize the CBBO parameters:

- *pMutation*: the mutation probability;
- *KeepRate*: parameter to keep elites from prior iteration to the next;
- N_H : the number of habitats (population size);
- c_1 and c_2 : the parameters of migration operator;
- α : the parameter of mutation operator;

As it mentioned previously, the value of parameters *pMutation* and *KeepRate* are set to 0.1 in all design examples. So, in CBBO algorithm, N_H , c_1 , c_2 and α are the internal parameters that should be controlled.

Step 2: Initialize habitats with randomly generated N_H habitats and evaluate fitness (HSI) for each habitat.

Step 3: For each individual, map the HSI to the number of species and calculate the immigration rate λ and the emigration rate μ for each habitat.

Step 4: Update the position of each habitat by the migration and mutation operators and evaluate them.

Step 5: Combine the elites from previous iteration with new habitats and select N_H habitats with high HSI among them.

Step 6: Repeat from Steps 3 to 6 till the termination criterion is met.

For other algorithms and comparative studies the interested reader may refer to [31–33].

4 Design examples

In this section, five design examples are studied to assess the performance of the CBBO approach for the optimization of truss structures with natural frequency constraints: 10-bar planar truss, the simply supported 37-bar planar truss, 52-bar space truss, 120-bar dome truss and 200-bar planar truss. Examples 1, 4 and 5 focus on optimal design of truss structures considering only size variables, while examples 2 and 3 discuss the weight minimization of truss structures considering both size and shape variables together. The performance of the CBBO may depend on some internal parameters such as number of habitats N_H , constant parameters c_1 , c_2 and α . In each design example, sensitivity analysis was performed for internal parameters of the CBBO algorithm to investigate how the CBBO is affected by these parameters and the best combination of them obtained. The sensitivity analyses are carried out on the CBBO

using different values of population size (N_H) and three constant parameters (c_1 , c_2 and α). For design examples 1 through 4, three settings are considered for N_H parameter and two settings for C_1 , C_2 and α parameters. That is, $N_H \in \{20, 30, 40\}$, $(c_1, c_2) \in \{1, 2\}$ and $\alpha \in \{0.05, 0.15\}$. For last design example the case of $N_H = 50$ is added to parameter setting cases. The proposed method were run 10 times with random initial population for each case of parameter combination and the best, worst, mean structural weights and standard deviations are obtained.

In order to assess the effect of different initial solution vector (i.e. initial population and initial values of y_0 and z_0) on the final result and because of the random nature of the algorithm, each design example are independently optimized 20 times with selected parameters by sensitivity analysis. The best result, average and the standard deviation of 20 independent runs are given in the tables.

Each run stops when the maximum iterations are reached. In all design examples, the maximum iterations are set to 200. In order to show effectiveness of the proposed algorithm, CBBO is compared with both standard BBO algorithm and other optimization methods in literature. It is worth mentioning that the same parameters are used for standard BBO and CBBO algorithms in all design examples. The CBBO and BBO implementation was coded in Matlab program

Example 1. A 10-bar planar truss

The first design example is the size optimization of a 10-bar planar truss with fixed configuration shown in Fig. 6. The Young's modulus and material density of truss members are 6.89×10^{10} kg/m² and 2770.0 kg/m³, respectively. As seen in Fig. 6 a non-structural mass of 454.0 kg are attached for all free nodes. The lower and upper bounds for the cross-sectional areas are specified as 0.645 cm² and 50 cm², respectively. In this design example, the three natural frequency constraints are considered as: $\omega_1 \geq 7$ Hz, $\omega_2 \geq 15$ Hz, $\omega_3 \geq 20$ Hz. It should be noted that in some references the Young's modulus of truss members is given as 6.98×10^{10} kg/m². So, for a fair comparison, two cases are considered as: $E = 6.89 \times 10^{10}$ kg/m² (Case 1) and $E = 6.98 \times 10^{10}$ kg/m² (Case 2).

The results of the sensitivity analysis carried out to find the best combination of the parameters for CBBO are presented in Tab. 1. It is apparent from Tab. 1 that $N_H = 30$, $c_1 = 1$, $c_2 = 1$ and $\alpha = 0.05$ are the relatively best case of parameter settings for Case 1 of this example. The results obtained by standard BBO and CBBO for two cases are summarized in Tab. 2 and compared to those reported previously.

From Tab. 2, in Case 1, it can be concluded that CBBO gives lightest design as compared to the results obtained by Grandhi and Venkayya [2], Sedaghati and et al. [3], Wang et al. [5] and Lingyun et al. [10], but slightly heavier design than DPSO [12] method. Also it is clear that the values of mean weight and standard deviation for CBBO are relatively less than other methods.

In Case 2, the results obtained by the standard BBO and

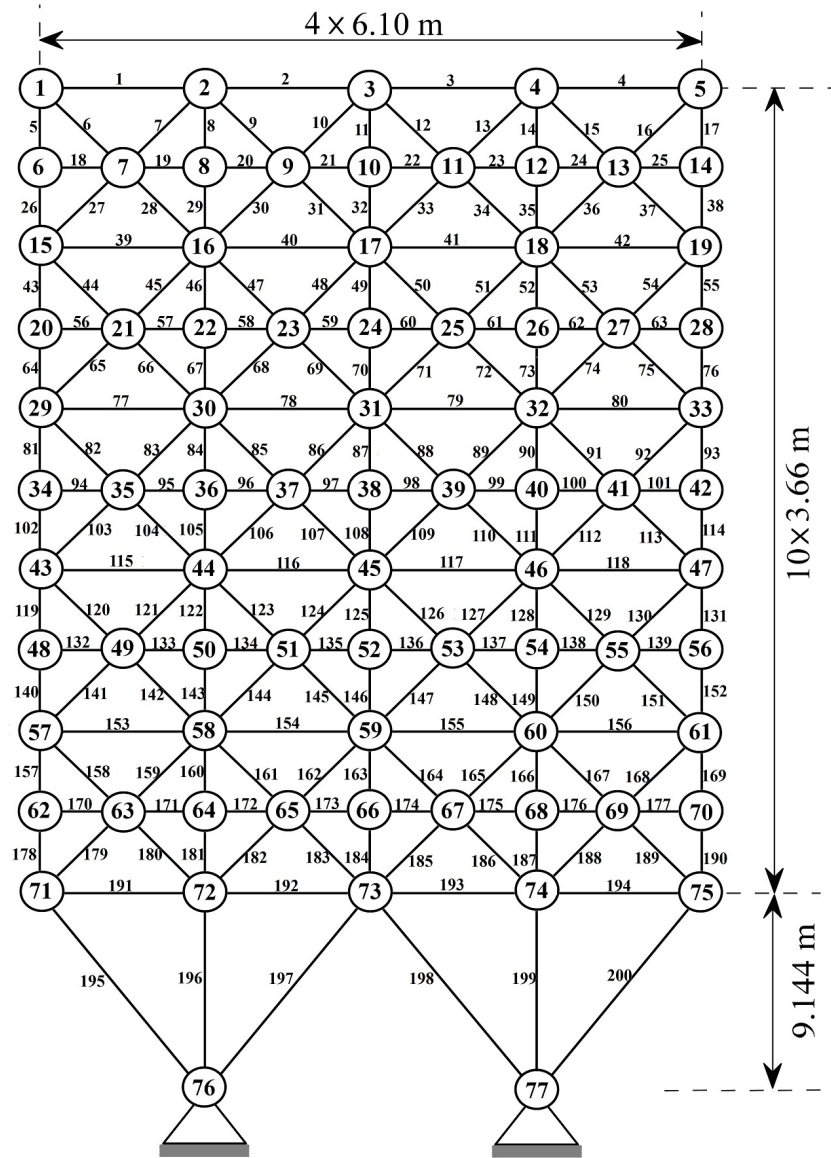


Fig. 6. Schematic of the planar 10-bar truss structure.

Tab. 1. Results of sensitivity analysis carried out to find the best combination of the parameters of CBBO for the planar 10-bar truss problem (Case 1).

Case	Parameters				Weight (kg)			
	N_H	c_1	c_2	α	Best	Mean	Std	Worst
1	20	1	1	0.05	533.68	539.21	3.79	545.77
2	20	2	1	0.05	535.75	542.58	4.12	547.47
3	20	1	2	0.05	534.41	540.55	4.21	547.72
4	30	1	1	0.05	532.47	535.49	3.49	541.55
5	30	2	1	0.05	532.96	538.52	3.85	542.84
6	30	1	2	0.05	534.88	539.84	3.40	543.49
7	40	1	1	0.05	533.08	535.89	3.11	542.37
8	40	2	1	0.05	533.73	537.32	3.10	542.12
9	40	1	2	0.05	534.81	541.51	3.46	546.52
10	20	1	1	0.5	534.42	538.45	3.50	543.41
11	20	2	1	0.5	538.21	546.88	7.61	560.15
12	20	1	2	0.5	537.38	546.37	6.94	561.01
13	30	1	1	0.5	533.80	537.07	3.26	545.24
14	30	2	1	0.5	537.54	542.82	3.48	549.04
15	30	1	2	0.5	535.1	544.39	4.94	552.69
16	40	1	1	0.5	533.91	538.02	3.81	545.34
17	40	2	1	0.5	539.74	544.24	3.56	550.93
18	40	1	2	0.5	535.33	541.39	4.27	548.29

Tab. 2. Optimized designs (cm^2) obtained for the 10-bar planar truss problem (the optimized weight does not include the added masses).

Design variable	Case 1					Case 2							
	Gran- dhi and Ven- kayya [2]	Seda- ghati et al. [3]	Wang et al. [5]	Lin- gyun et al. [10]	Kaveh and Zol- ghadr [12]	Present work		Gomes [11]	Kaveh and Zolghadr [13]			Present work	
				NHPGA	DPSO	BBO	CBBO	PSO	CSS	En- hanced CSS	CSS- BBBC	BBO	CBBO
A_1	36.584	38.245	32.456	42.234	35.944	42.220	35.897	37.712	38.811	39.569	35.274	41.524	34.895
A_2	24.658	9.916	16.577	18.555	15.530	16.336	15.071	9.959	9.031	16.740	15.463	16.94	14.359
A_3	36.584	38.619	32.456	38.851	35.285	31.854	35.171	40.265	37.099	34.361	32.110	35.048	34.946
A_4	24.658	18.232	16.577	11.222	15.385	18.418	14.804	16.788	18.479	12.994	14.065	8.3278	14.541
A_5	4.167	4.419	2.115	4.783	0.648	0.734	0.645	11.576	4.479	0.645	0.645	3.765	0.645
A_6	2.070	4.419	4.467	4.451	4.583	4.831	4.6946	3.955	4.205	4.802	4.880	4.5674	4.5984
A_7	27.032	20.097	22.810	21.049	23.610	21.757	24.094	25.308	20.842	26.182	24.046	24.932	23.818
A_8	27.032	24.097	22.810	20.949	23.599	23.581	24.056	21.613	23.023	21.260	24.340	21.182	24.057
A_9	10.346	13.890	17.490	10.257	13.135	12.771	12.986	11.576	13.763	11.766	13.343	12.229	12.402
A_{10}	10.346	11.452	17.490	14.342	12.357	12.104	12.358	11.186	11.414	11.392	13.543	13.256	12.646
Weight (kg)	594	537.01	553.8	542.75	532.39	541.32	532.47	537.98	531.95	529.25	529.09	535.73	524.60
Mean weight (kg)	N/A	N/A	N/A	552.447	537.8	553.57	537.01	540.89	536.39	538.53	N/A	551.76	527.23
Standard deviation (kg)	N/A	N/A	N/A	4.864	4.02	7.64	3.90	6.84	3.32	5.97	N/A	11.92	2.52

CBBO are compared with those reported in the literature like PSO [11], CSS, Enhanced CSS and CSS-BBBC [13]. It is observed from Tab. 2 that the CBBO significantly outperforms other methods in terms of the values of best, mean and standard deviation of structural weight. In addition, the mean weight obtained by CBBO is also lighter than the best weights presented by other methods, which shows its accomplishment in reaching the near-optimal design. Moreover, it should be noted that Kaveh and Zolghadr [12] obtained a weight of 524.70 kg for Case 2 which is heavier than the weight obtained by CBBO.

The natural frequencies evaluated at the optimum designs for each case are given in Tab. 3. In addition, the convergence behaviors of the best solution and the average of 20 independent runs for each case are shown in Fig. 7. It is clear from Fig. 7 that the CBBO converges to the near-optimum solution after 80 iterations without any abrupt oscillations, while standard BBO method converges to local solution as a result of suffering from the shortcoming of premature convergence. The CBBO reached the best result in iterations 120 and 113 for Case 1 and Case 2, respectively.

Example 2. A simply supported 37-bar planar truss

The second design example deals with the size and shape optimization of a simply supported 37-bar planar truss shown in Fig. 8. The Young's modulus and material density of truss members are 2.1×10^{11} N/m² and 7800 kg/m³, respectively. As seen in Fig. 8, a non-structural mass of 10 kg are attached for all free nodes. The constant rectangular cross-sectional areas of 4×10^{-3} m² are specified for all members of the lower chord and the cross-sectional areas of other members are considered as design variables. In addition, the y-coordinate of upper nodes are taken as layout variables considering symmetry and their vertical position must not exceed ± 1.5 m. Thus, the optimization problem includes 19 design variables (5 for shape variables and 14 for size variables). Furthermore, the structure is subject to the first three frequency constraints as: $\omega_1 \geq 20$ Hz, $\omega_2 \geq 40$ Hz, $\omega_3 \geq 60$ Hz.

The results of the sensitivity analysis carried out to find the best combination of parameters for CBBO are reported in Tab. 4. Once again, it can be seen from Tab. 4 that the minimum structural weight is obtained for $N_H = 30$, $c_1 = 1$, $c_2 = 1$ and $\alpha = 0.05$.

In Tab. 5, the results obtained by the CBBO and BBO are compared with those reported in the literature like NHGA [10], PSO [11], CSS, enhanced CSS [29] and DPSO [12]. From this table, it can be observed that CBBO significantly outperforms other methods in terms of the values of best, mean and standard deviation, which shows its stability in reaching the optimal weight of the structure during 20 independent runs. It is evident from Tab. 5 that the structural weight and standard deviation of 20 independent runs for the CBBO are 360.29 kg and 0.67 kg, respectively, which are much less than the other optimization algorithms. Also, the natural frequencies obtained at the optimum designs are presented in Tab. 6.

Fig. 9 compares the optimized layout with the initial configuration of the structure.

The convergence diagrams of the best solution and the average of 20 independent runs are presented in Fig. 10. As seen, the convergence rates of the best run and the average of 20 independent runs are close together which represents smaller value of the standard deviation.

Example 3. A 52-bar space truss

A 52-bar space truss shown in Fig. 11 is the third design example. The Young's modulus and material density of truss members are 2.1×10^{11} kg/m² and 7800 kg/m³, respectively. A non-structural mass of 50 kg are attached for all free nodes. As seen in Tab. 7, the elements of the structure are categorized in 8 groups with respect to symmetry. The coordinates of all free nodes are taken as design variables considering symmetry and their position movements must not exceed ± 2 m in x and z directions. The lower and upper bounds for the cross-sectional areas are specified as 1 cm² and 10 cm², respectively. Therefore, the optimization problem includes 13 design variables (5 shape variables and 8 size variables). Furthermore, the structure is subject to the first two frequency constraints as: $\omega_1 \leq 15.916$ Hz, $\omega_2 \geq 28.648$ Hz.

Again, Tab. 8 presents the results of the sensitivity analysis carried out to find the best combination of parameters for CBBO. The best optimal structural weight is obtained for $N_H = 40$, $c_1 = 2$, $c_2 = 1$ and $\alpha = 0.05$.

The optimal nodal coordinates and cross-sectional areas obtained by the CBBO, BBO and the other optimization methods recently published in literature are reported in Tab. 9. It is quite evident that CBBO gives the lightest design than all other techniques in the literature based on Tab. 9. From Tab. 9, it can be concluded that CBBO gives small mean weight as compared to CSS [29], Enhanced CSS [29], CSS-BBBC [13], PSO [11], NHGA [10] and Lin et al. [34], but slight large mean weight when compared with the DPSO [12] method. However, it should be noted that the CBBO produces much smaller overall standard deviation than all other methods. Also, the natural frequencies obtained at the optimum designs are presented in Tab. 10.

Tab. 11 compares the optimized shape with the initial layout of the structure. In addition, the convergence characteristics of the CBBO and BBO are shown in Tab. 12.

Example 4. A 120-bar dome truss

The fourth design example is the size optimization of a 120-bar dome truss shown in Fig. 14. The members of the structure are divided into 7 groups using symmetry as shown in Fig. 14. The minimum and maximum cross-sectional area for each group of members is 1 cm² and 129.3 cm², respectively. The Young's modulus and material density of truss members are 2.1×10^{11} kg/m² and 7971.810 kg/m³, respectively. Non-structural masses are attached to all free nodes as follows: 3000 kg at node one, 500 kg at nodes 2 through 13 kg and 100 kg at the rest of the nodes. Furthermore, the structure is subject to the first two frequency constraints as: $\omega_1 \geq 9$ Hz, $\omega_2 \geq 11$ Hz.

Tab. 3. Natural frequencies (Hz) evaluated at the optimized designs for the 10-bar planar truss.

Fre- quency No.	Case 1					Case 2							
	Gran- dhi and Ven- kayya [2]	Seda- ghati et al. [3]	Wang et al. [5]	Lin- gyun et al. [10]	Kaveh and Zol- ghadr [12]	Present work		Gomes [11]	Kaveh and Zolghadr [13]		Present work		
				NHPGA	DPSO	BBO	CBBO	PSO	CSS	En- hanced CSS	CSS- BBBC	BBO	CBBO
1	7.059	6.992	7.011	7.008	7.000	7.000	7.000	7.000	7.000	7.000	7.000	7.001	7.000
2	15.895	17.599	17.302	18.148	16.187	16.473	16.179	17.786	17.442	16.238	16.119	16.945	16.166
3	20.425	19.973	20.001	20.000	20.000	20.042	20.004	20.000	20.031	20.000	20.075	20.040	20.001
4	20.425	19.977	20.100	20.508	20.021	20.585	20.091	20.063	20.208	20.361	20.457	20.435	20.012
5	20.425	28. 173	30.869	27.797	28.470	28.396	28.558	27.776	28.261	28.121	29.149	28.399	28.644
6	30.189	31.029	32.666	31.281	29.243	29.312	29.078	30.939	31.139	28.610	29.761	30.881	28.998
7	54.286	47.628	48.282	48.304	48.769	49.883	48.516	47.297	47.704	48.390	47.950	46.282	48.396
8	56.546	52.292	52.306	53.306	51.389	53.031	51.074	52.286	52.420	52.291	51.215	52.699	50.896

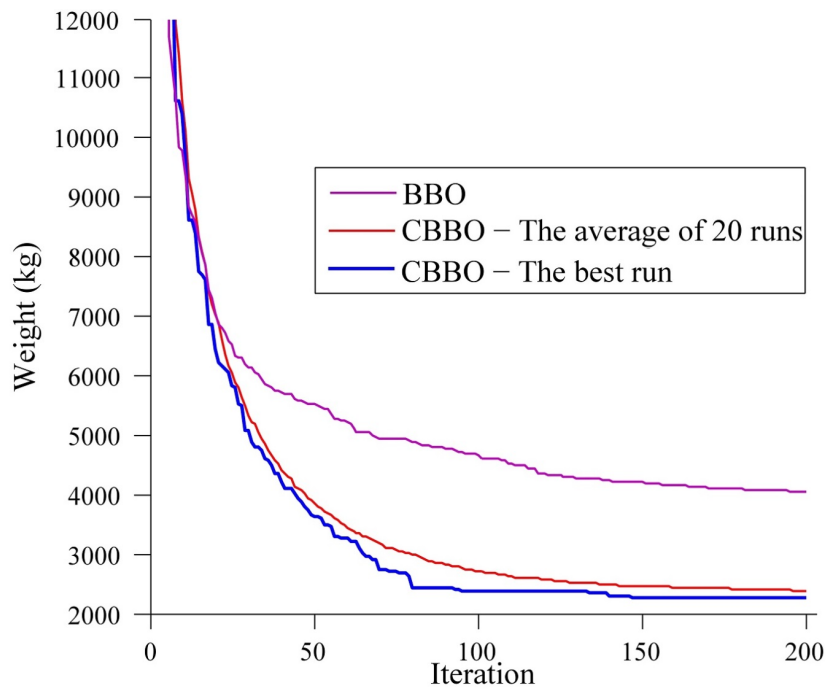


Fig. 7. Comparative convergence behaviors of the standard BBO and CBBO algorithms for 10-bar planar truss.

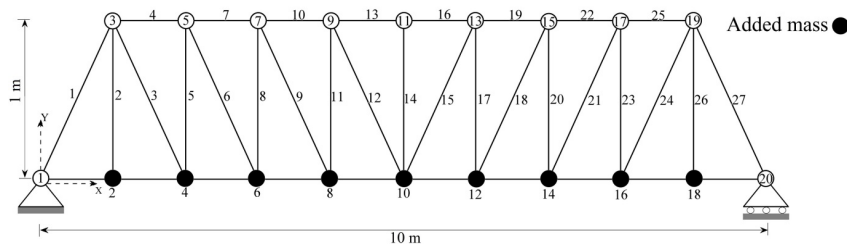


Fig. 8. Schematic of the simply-supported planar 37-bar truss.

Tab. 4. Results of sensitivity analysis for best combination of the parameters of CBBO for the 37-bar planar truss problem.

Case	N_H	Parameters			Weight (kg)			
		c_1	c_2	α	Best	Mean	Std	Worst
1	20	1	1	0.05	360.85	362.02	1.00	364.49
2	20	2	1	0.05	361.86	364.21	2.13	368.79
3	20	1	2	0.05	361.91	363.79	2.24	369.49
4	30	1	1	0.05	360.29	361.11	0.48	362.21
5	30	2	1	0.05	361.63	362.73	0.95	364.57
6	30	1	2	0.05	361.44	363.56	2.44	367.47
7	40	1	1	0.05	360.44	361.15	0.33	361.64
8	40	2	1	0.05	361.05	362.74	1.06	364.32
9	40	1	2	0.05	361.83	362.77	1.32	366.32
10	20	1	1	0.5	361.70	363.60	1.46	367.03
11	20	2	1	0.5	364.58	367.51	1.68	370.28
12	20	1	2	0.5	363.70	366.65	2.20	369.97
13	30	1	1	0.5	361.24	363.10	1.10	364.90
14	30	2	1	0.5	363.01	365.23	1.63	368.18
15	30	1	2	0.5	363.94	366.21	2.60	372.83
16	40	1	1	0.5	362.30	363.16	0.42	363.70
17	40	2	1	0.5	361.70	364.16	1.67	367.04
18	40	1	2	0.5	362.95	365.98	1.95	369.28

Tab. 5. Optimized designs for the 37-bar planar truss problem; optimal nodal coordinates (Y_i (m)) and cross-sectional areas A_i (cm²).

Design variable	Wang et al. [5]	Lingyun et al. [10]	Gomes [11]	Kaveh and Zolghadr [12, 29]			Present work	
				NHGA	PSO	CSS	Enhanced CSS	DPSO
Y_3, Y_{19}	1.2086	1.1998	0.9637	0.8726	1.0289	0.9482	0.94404	0.9794
Y_5, Y_{17}	1.5788	1.6553	1.3978	1.2129	1.3868	1.3439	1.25010	1.3411
Y_7, Y_{15}	1.6719	1.9652	1.5929	1.3826	1.5893	1.5043	1.39930	1.5403
Y_9, Y_{13}	1.7703	2.0737	1.8812	1.4706	1.6405	1.6350	1.54140	1.6861
Y_{11}	1.8502	2.3050	2.0856	1.5683	1.6835	1.7182	1.56390	1.7661
A_1, A_{27}	3.2508	2.8932	2.6797	2.9082	3.4484	2.6208	3.82130	2.6334
A_2, A_{26}	1.2364	1.1201	1.1568	1.0212	1.5045	1.0397	1.01400	1.0787
A_3, A_{24}	1.0000	1.0000	2.3476	1.0363	1.0039	1.0464	1.83660	1.0000
A_4, A_{25}	2.5386	1.8655	1.7182	3.9147	2.5533	2.7163	2.92040	2.5520
A_5, A_{23}	1.3714	1.5962	1.2751	1.0025	1.0868	1.0252	1.09570	1.1357
A_6, A_{21}	1.3681	1.2642	1.4819	1.2167	1.3382	1.5081	1.13920	1.2483
A_7, A_{22}	2.4290	1.8254	4.685	2.7146	3.1626	2.3750	3.25890	3.1168
A_8, A_{20}	1.6522	2.0009	1.1246	1.2663	2.2664	1.4498	1.42990	1.4849
A_9, A_{18}	1.8257	1.9526	2.1214	1.2668	1.4499	1.51360	1.4634	
A_{10}, A_{19}	2.3022	1.9705	3.86	4.0274	1.7518	2.5327	4.01820	2.4885
A_{11}, A_{17}	1.3103	1.8294	2.9817	1.3364	2.7789	1.2358	2.67270	1.2502
A_{12}, A_{15}	1.4067	1.2358	1.2021	1.0548	1.4209	1.3528	1.18160	1.3661
A_{13}, A_{16}	2.1896	1.4049	1.2563	2.8116	1.0100	2.9144	2.40820	2.1451
A_{14}	1.0000	1.0000	3.3276	1.1702	2.2919	1.0085	1.22720	1.0000
Weight (kg)	366.5	368.84	377.20	362.84	362.38	360.40	369.10	360.29
Mean weight (kg)	N/A	378.8259	381.2	366.77	365.75	362.21	377.40	361.33
Standard deviation (kg)	N/A	9.0325	4.26	3.742	3.461	1.68	7.35	0.67

Tab. 6. Natural frequencies (Hz) evaluated at the optimized designs for the simply supported 37-bar planar truss.

Frequency No.	Wang et al. [5]	Lingyun et al. [10]	Gomes [11]	Kaveh and Zolghadr [12,29]			Present work	
				NHGA	PSO	CSS	Enhanced CSS	DPSO
1	20.0850	20.0013	20.0001	20.0000	20.0028	20.0194	20.3110	20.029
2	42.0743	40.0305	40.0003	40.0693	40.0155	40.0113	42.8990	40.013
3	62.9383	60.0000	60.0001	60.6982	61.2798	60.0082	62.1780	60.028
4	74.4539	73.0444	73.0440	75.7339	78.1100	76.9896	79.0920	76.811
5	90.0576	89.8244	89.8240	97.6137	98.4100	97.2222	103.0100	96.862

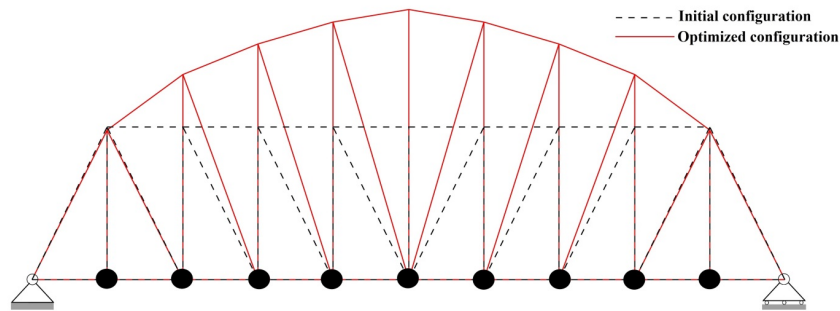


Fig. 9. Comparison of the optimized shape with the initial configuration of the simply-supported planar 37-bar truss.

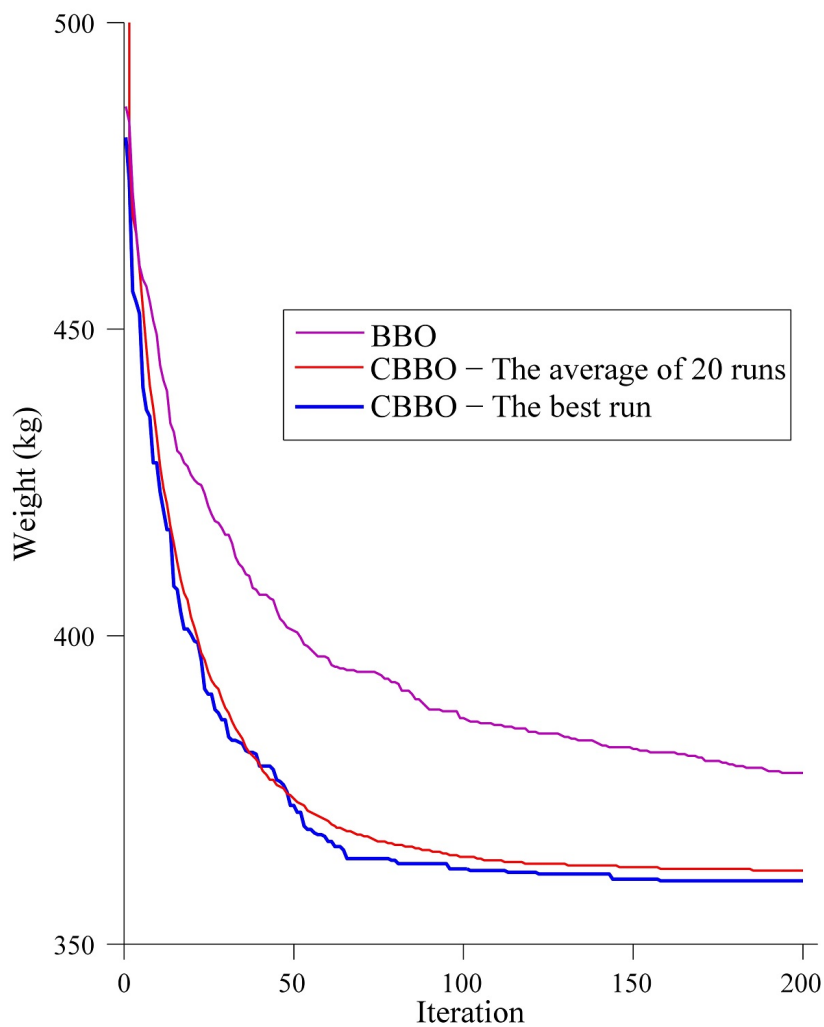


Fig. 10. Comparison of convergence diagrams of standard BBO and CBBO algorithms for the simply-supported planar 37-bar truss.

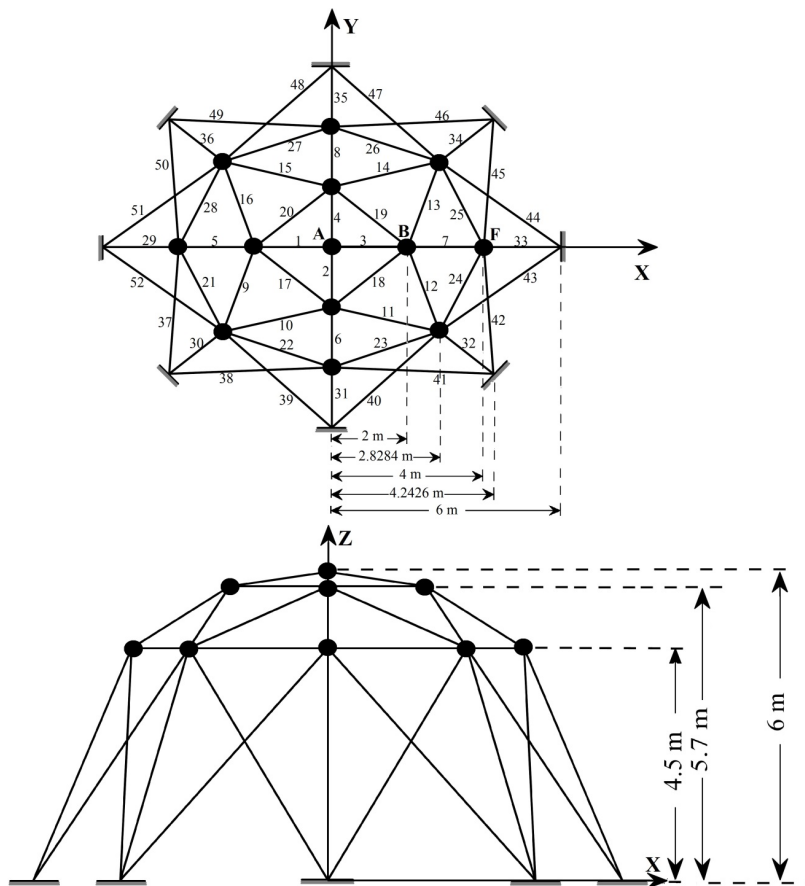


Fig. 11. Schematic of the initial layout of the spatial 52-bar space truss: (a) Top view (b) Side view.

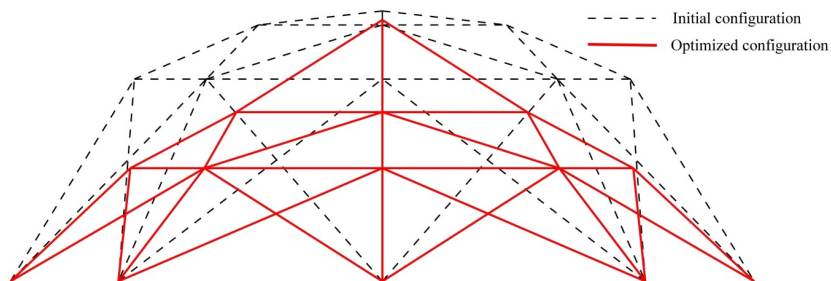


Fig. 12. Comparison of the optimized shape with the initial configuration of the 52-bar space truss.

Tab. 7. Element grouping adopted in the 52-bar space truss problem.

Group number	Elements
1	1, 2, 3, 4
2	5, 6, 7, 8
3	9, 10, 11, 12, 13, 14, 15, 16
4	17, 18, 19, 20
5	21, 22, 23, 24, 25, 26, 27, 28
6	29, 30, 31, 32, 33, 34, 35, 36
7	37, 38, 39, 40, 41, 42, 43, 44
8	45, 46, 47, 48, 49, 50, 51, 52

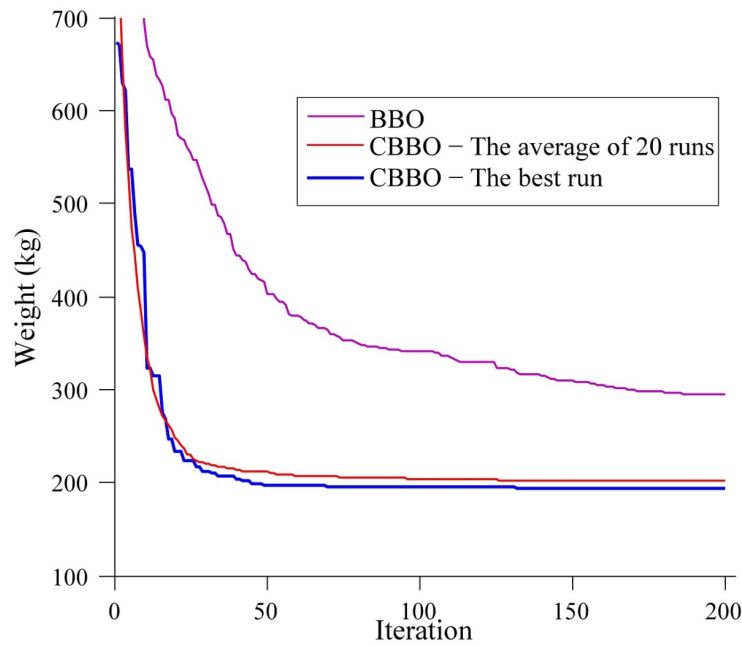


Fig. 13. Comparison of convergence curves of standard BBO and CBBO algorithms for the 52-bar space truss.

Tab. 8. Results of sensitivity analysis carried out to find the best combination of the parameters of CBBO for the 52-bar space truss problem.

Case	N_H	Parameters			Weight (kg)			
		c_1	c_2	α	Best	Mean	Std	Worst
1	20	1	1	0.05	198.94	220.12	15.67	239.46
2	20	2	1	0.05	195.65	229.46	50.14	330.67
3	20	1	2	0.05	199.37	230.76	37.65	313.78
4	30	1	1	0.05	204.63	227.75	34.15	316.42
5	30	2	1	0.05	194.90	208.03	10.20	226.01
6	30	1	2	0.05	196.49	206.97	13.50	242.73
7	40	1	1	0.05	204.11	219.72	17.06	254.88
8	40	2	1	0.05	194.09	199.83	4.06	206.53
9	40	1	2	0.05	194.73	201.93	12.11	235.25
10	20	1	1	0.5	206.21	244.34	55.23	393.03
11	20	2	1	0.5	200.85	225.81	28.16	289.23
12	20	1	2	0.5	205.36	240.00	42.64	329.92
13	30	1	1	0.5	205.13	228.69	28.67	305.79
14	30	2	1	0.5	199.90	216.39	26.79	291.87
15	30	1	2	0.5	198.79	213.17	19.13	265.7
16	40	1	1	0.5	199.70	210.01	11.35	238.10
17	40	2	1	0.5	201.89	210.85	8.65	232.41
18	40	1	2	0.5	199.38	211.31	9.73	232.11

Tab. 9. Optimized designs obtained for the 52-bar space truss problem ; optimal nodal coordinates and cross-sectional areas.

Design variable	Lin et al. [30]	Lingyun et al. [10]	Gomes [11]	Kaveh and Zolghadr [12, 13, 29]			Present work		
		NHGA	PSO	CSS	Enhanced CSS	CSS-BBBC	DPSO	BBO	CBBO
Z_A (m)	4.3201	5.8851	5.5344	5.2716	6.1590	5.3310	6.1123	5.4611	5.8162
X_B (m)	1.3153	1.7623	2.0885	1.5909	2.2609	2.1340	2.2343	1.5177	2.3525
Z_B (m)	4.1740	4.4091	3.9283	3.7093	3.9154	3.7190	3.8321	4.0582	3.7684
X_F (m)	2.9169	3.4406	4.0255	3.5595	4.0836	3.9350	4.0316	3.5204	4.0484
Z_F (m)	3.2676	3.1874	2.4575	2.5757	2.5106	2.5000	2.5036	2.7484	2.5000
A_1 (cm ²)	1.0000	1.0004	0.3696	1.0464	1.0335	1.0000	1.0001	1.5196	1.0000
A_2 (cm ²)	1.3300	2.1417	4.1912	1.7295	1.0960	1.3056	1.1397	1.1760	1.0000
A_3 (cm ²)	1.5800	1.4858	1.5123	1.6507	1.2449	1.4230	1.2263	1.1046	1.1836
A_4 (cm ²)	1.0000	1.4018	1.5620	1.5059	1.2358	1.3851	1.3335	1.5884	1.5035
A_5 (cm ²)	1.7100	1.9116	1.9154	1.7210	1.4078	1.4226	1.4161	1.0948	1.3967
A_6 (cm ²)	1.5400	1.0109	1.1315	1.0020	1.0022	1.0000	1.0001	1.1219	1.0000
A_7 (cm ²)	2.6500	1.4693	1.8233	1.7415	1.6024	1.5562	1.5750	2.5201	1.5787
A_8 (cm ²)	2.8700	2.1411	1.0904	1.2555	1.4596	1.4485	1.4357	1.8206	1.4103
Weight (kg)	298.00	236.050	228.380	205.237	197.337	197.309	195.351	232.36	194.09
Mean weight (kg)	N/A	274.164	234.3	213.101	205.617	N/A	198.71	294.48	201.27
Standard deviation (kg)	N/A	37.462	5.22	7.391	6.924	N/A	13.85	39.76	4.93

Tab. 10. Natural frequencies (Hz) evaluated at the optimal designs for the 52-bar space truss.

Frequency No.	Lin et al. [32]	Lingyun et al. [10]	Gomes [11]	Kaveh and Zolghadr [12, 13, 29]			Present work		
		NHGA	PSO	CSS	Enhanced CSS	CSS-BBBC	DPSO	BBO	CBBO
1	15.2196	12.8051	12.751	9.246	11.849	12.987	11.3150	9.3486	12.796
2	29.2837	28.6489	28.649	28.648	28.649	28.648	28.6480	28.6540	28.649
3	29.2837	28.6489	28.649	28.699	28.659	28.679	28.6480	28.6610	28.649
4	31.6847	29.5398	28.803	28.735	28.718	28.713	28.6500	28.6610	28.656
5	33.1547	30.2443	29.230	29.223	29.192	30.262	28.6880	29.5260	29.663

Tab. 11. Optimized designs (cm²) obtained for the 120-bar dome truss problem.

Element group	Kaveh and Zolghadr [13, 15]			Present work		
	CSS	CSS-BBBC	PSO	DPSO	BBO	CBBO
1	21.710	17.478	23.494	19.6070	19.9850	19.8120
2	40.862	49.076	32.976	41.2900	34.8660	38.9570
3	9.048	12.365	11.492	11.1360	16.8660	10.1770
4	19.673	21.979	24.839	21.0250	21.9560	21.1170
5	8.336	11.190	9.964	10.0600	15.1220	10.2610
6	16.120	12.590	12.039	12.7580	9.8383	12.4840
7	18.976	13.585	14.249	15.4140	16.5440	14.9530
Weight (kg)	9204.51	9046.34	9171.93	8890.48	9427.18	8727.40
Mean weight (kg)	N/A	N/A	9251.84	8895.99	9763.32	8769.40
Standard deviation (kg)	N/A	N/A	89.38	4.26	674.77	37.52

Tab. 12. Natural frequencies (Hz) evaluated at the optimized designs for the 120-bar dome truss.

Frequency number	Kaveh and Zolghadr [12, 13]				Present work	
	CSS	CSS-BBBC	PSO	DPSO	BBO	CBBO
1	9.002	9.000	9.0000	9.0001	9.0331	9.0006
2	11.002	11.007	11.0000	11.0007	11.0732	11.0020
3	11.006	11.018	11.0052	11.0053	11.0732	11.0020
4	11.015	11.026	11.0134	11.0129	11.1359	11.0160
5	11.045	11.048	11.0428	11.0471	11.2118	11.0860

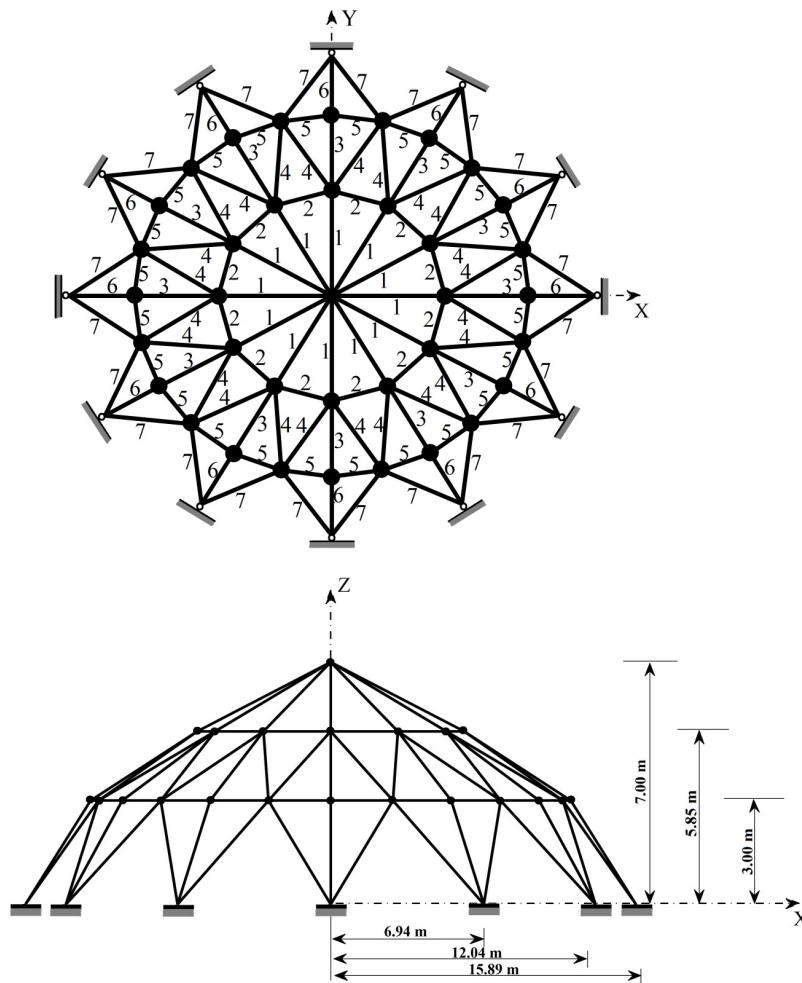


Fig. 14. Schematic of the 120-bar dome truss.

Once again, the results of the sensitivity analysis carried out to find the best combination of parameters for CBBO are reported in Tab. 13. In this design example, it can be seen from Tab. 13 that the lowest structural weight is obtained for $N_H = 40$, $c_1 = 1$, $c_2 = 1$ and $\alpha = 0.05$

The optimization results obtained by the standard BBO and CBBO are presented in Tab. 11 and are compared with those of the CSS [15], CSS-BBBC [15], PSO [13] and DPSO [13] approaches. It is quite evident that CBBO significantly outperforms other algorithms in terms of minimum weight, mean and standard deviation. On the other hand, the mean gained by the CBBO is also better than the best weights obtained by other methods as provided in Tab. 11. It means that the CBBO algorithm obtained better design and lightest weight in all 20 independent runs. In addition, the natural frequencies obtained at the optimum designs are presented in Tab. 12.

The convergence behaviors of the best solution and the average of 20 independent runs are presented in Fig. 15. As it can be seen from Fig. 15 that the best result is obtained after 120 iterations and it is clear that the performance of the proposed algorithm confirms the validity of the developed approach.

Example 5. A 200-bar planar truss

The last design example is the size optimization of a 200-bar planar truss shown in Fig. 16. The Young's modulus is 2.1×10^{11} kg/m² and the material density of truss members is 7860 kg/m³. The minimum permitted cross-sectional area for the truss members is taken as 0.1 cm². A non-structural mass of 100 kg are attached for all free nodes. Furthermore, the structure is subject to the first three frequency constraints as: $\omega_1 \geq 5$ Hz, $\omega_2 \geq 10$ Hz, $\omega_3 \geq 15$ Hz. The members of the structure are divided into 29 groups as shown in Tab. 14. Hence, the optimization problem includes 19 design variables and it is relatively high dimensional optimization problem. Kaveh and Zolghadr [12] used this design example to size optimization with frequency constraints.

Another sensitivity analysis is carried out to find the best combination of internal parameters of the CBBO. In this design example, six cases of parameter settings are considered with the number of fifty habitats ($N_H = 50$), due to high dimensionality of the optimization problem. From Tab. 15 it can be observed that the lightest structural weight for this structure is obtained by $N_H = 50$, $c_1 = 1$, $c_2 = 1$ and $\alpha = 0.05$

Tab. 16 summarizes the optimal results obtained by both the standard BBO and CBBO algorithms. The results are compared with those CSS [12] and CSS-BBBC [12] approaches. Once again, it is evident that CBBO yields lighter structural weight than CSS [12] and CSS-BBBC [12]. The weight obtained by CBBO is 35.65 kg lighter than the weight found by CSS-BBBC [12], which is relatively considerable.

The natural frequencies evaluated at optimum designs are given in Tab. 17.

In Fig. 17, the convergence behaviors of the average of 20 independent runs and the best run for CBBO are compared with

original BBO. Once again, it can be seen that CBBO can improve the performance of the original BBO and obtain the lightest weight.

Tab. 13. Results of sensitivity analysis carried out to find the best combination of the parameters of CBBO for the 120-bar dome truss problem.

Case	Parameters				Weight (kg)			
	N_H	c_1	c_2	α	Best	Mean	Std	Worst
1	20	1	1	0.05	8747.60	8810.30	45.04	8860.90
2	20	2	1	0.05	8752.00	8835.50	89.03	9037.70
3	20	1	2	0.05	8776.90	8896.60	116.69	9145.10
4	30	1	1	0.05	8734.80	8767.50	25.08	8812.20
5	30	2	1	0.05	8759.90	8838.70	61.43	8960.00
6	30	1	2	0.05	8745.80	8873.10	86.30	8994.50
7	40	1	1	0.05	8727.40	8767.70	41.00	8847.60
8	40	2	1	0.05	8735.90	8853.50	109.81	9085.40
9	40	1	2	0.05	8781.30	8866.3	71.26	8976.30
10	20	1	1	0.5	8852.40	8988.20	143.15	9255.50
11	20	2	1	0.5	8969.10	9224.60	192.49	9686.30
12	20	1	2	0.5	8927.40	9256.90	333.18	9934.40
13	30	1	1	0.5	8826.70	8918.70	67.95	9038.90
14	30	2	1	0.5	8819.00	8955.80	119.15	9218.90
15	30	1	2	0.5	8841.90	9136.00	280.52	9655.90
16	40	1	1	0.5	8807.70	8861.20	54.23	9005.70
17	40	2	1	0.5	8773.70	9030.00	134.72	9205.30
18	40	1	2	0.5	8867.50	8976.10	175.45	9416.60

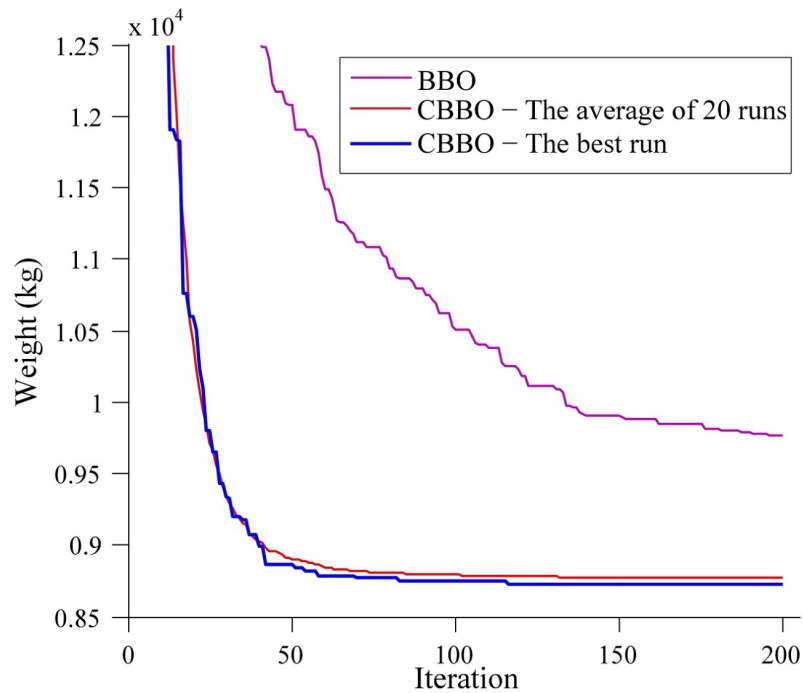


Fig. 15. Comparison of convergence diagrams of standard BBO and CBBO algorithms for the 120-bar dome truss.

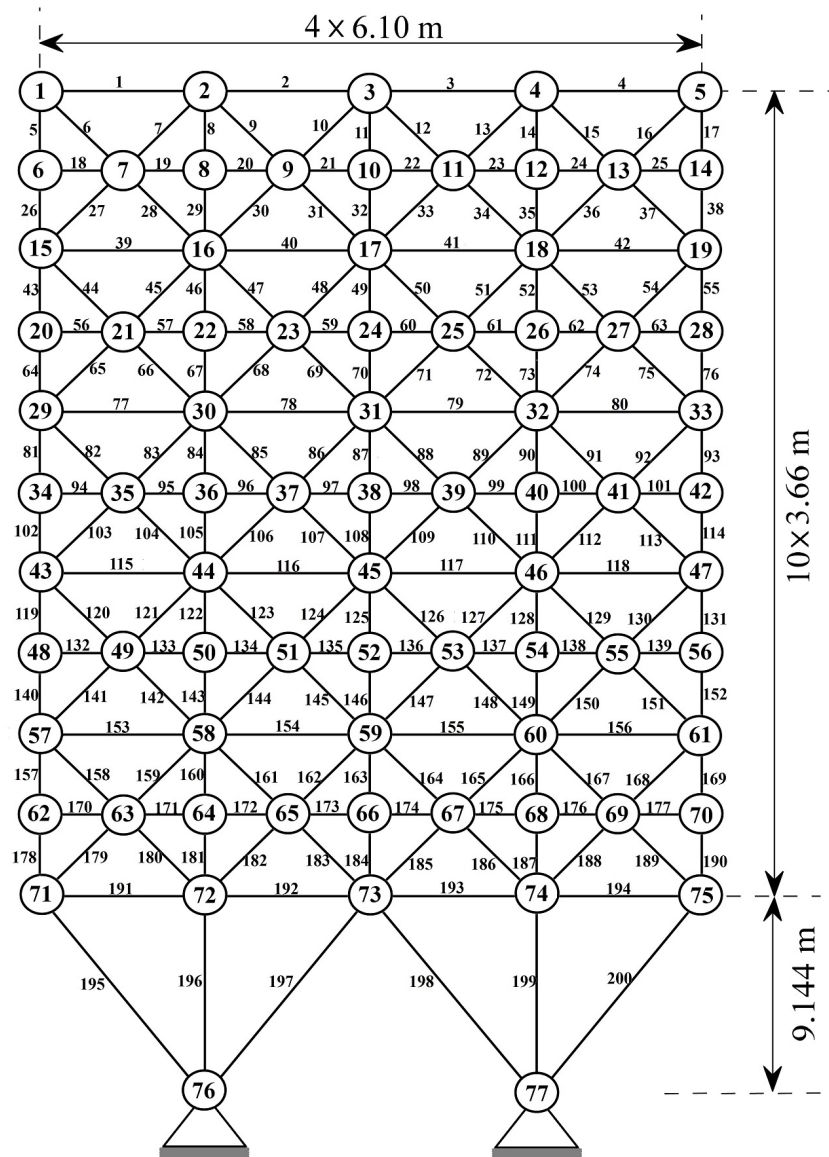


Fig. 16. Schematic of the 200-bar planar truss.

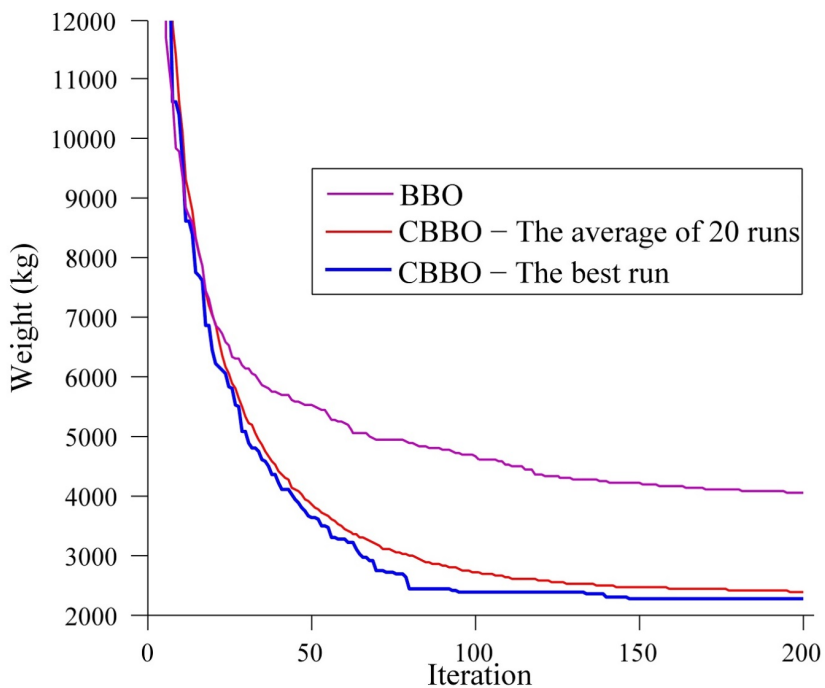


Fig. 17. Comparison of convergence curves of standard BBO and CBBO algorithms for the 200-bar planar truss.

Tab. 14. Elements grouping adopted in the 200-bar planar truss.

Group number	Members	Group number	Members
1	1, 2, 3, 4	15	102, 105, 108, 111, 114 82, 83, 85, 86, 88, 89, 91,
2	5, 8, 11, 14, 17	16	92, 103, 104, 106, 107, 109, 110, 112, 113
3	19, 20, 21, 22, 23, 24	17	115, 116, 117, 118
4	18, 25, 56, 63, 94, 101, 132, 139, 170, 177	18	119, 122, 125, 128, 131
5	26, 29, 32, 35, 38	19	133, 134, 135, 136, 137, 138
6	6, 7, 9, 10, 12, 13, 15, 16, 27, 28, 30, 31, 33, 34, 36, 37	20	140, 143, 146, 149, 152
7	39, 40, 41, 42	21	120, 121, 123, 124, 126, 127, 129, 130, 141, 142, 144, 145, 147, 148, 150, 151
8	43, 46, 49, 52, 55	22	153, 154, 155, 156
9	57, 58, 59, 60, 61, 62	23	157, 160, 163, 166, 169
10	64, 67, 70, 73, 76	24	171, 172, 173, 174, 175, 176
11	44, 45, 47, 48, 50, 51, 53, 54, 65, 66, 68, 69, 71, 72, 74, 75	25	178, 181, 184, 187, 190
12	77, 78, 79, 80	26	158, 159, 161, 162, 164, 165, 167, 168, 179, 180, 182, 183, 185, 186, 188, 189
13	81, 84, 87, 90, 93	27	191, 192, 193, 194
14	95, 96, 97, 98, 99, 100	28	195, 197, 198, 200
		29	196, 199

Tab. 15. Results of sensitivity analysis carried out to find the best combination of the parameters of CBBO for the 200-bar planar truss problem.

Case	N_H	Parameters			Weight (kg)			
		c_1	c_2	α	Best	Mean	Std	Worst
1	20	1	1	0.05	2583.60	3196.40	445.68	3839.50
2	20	2	1	0.05	2693.80	2976.40	216.92	3395.90
3	20	1	2	0.05	2764.70	2950.70	165.56	3251.80
4	30	1	1	0.05	2449.50	2571.00	98.16	2773.70
5	30	2	1	0.05	2421.60	2756.90	174.62	3019.10
6	30	1	2	0.05	2492.10	2753.10	225.90	3146.00
7	40	1	1	0.05	2365.20	2449.10	66.19	2574.40
8	40	2	1	0.05	2518.00	2663.90	98.50	2835.80
9	40	1	2	0.05	2405.30	2551.40	119.05	2744.60
10	50	1	1	0.05	2262.96	2364.10	86.54	2569.40
11	50	2	1	0.05	2421.60	2574.70	98.26	2709.80
12	50	1	2	0.05	2355.00	2496.60	66.06	2562.10
13	20	1	1	0.15	2717.60	3194.00	261.42	3682.80
14	20	2	1	0.15	3139.60	3760.10	423.68	4600.30
15	20	1	2	0.15	3052.90	3578.60	250.38	3887.90
16	30	1	1	0.15	2628.30	2844.20	128.58	3043.80
17	30	2	1	0.15	3277.10	3495.40	180.70	3817.20
18	30	1	2	0.15	3017.90	3314.80	240.64	3676.20
19	40	1	1	0.15	2502.50	2799.40	219.12	3166.70
20	40	2	1	0.15	2902.10	3433.20	331.16	3910.30
21	40	1	2	0.15	2900.10	3282.70	185.51	3552.80
22	50	1	1	0.15	2599.90	2693.40	84.50	2891.50
23	50	2	1	0.15	2893.10	3096.30	159.98	3321.70
24	50	1	2	0.15	2706.80	3137.00	254.49	3582.40

Tab. 16. Optimized designs (cm^2) obtained for the 200-bar planar truss problem.

Element group	Kaveh and Zolghadr [12]		Present work	
	CSS	CSS-BBBC	BBO	CBBO
1	1.2439	0.2934	2.1211	0.43194
2	1.1438	0.5561	2.8942	0.42188
3	0.3769	0.2952	2.7893	0.12477
4	0.1494	0.1970	0.9380	0.19263
5	0.4835	0.8340	2.0888	0.69798
6	0.8103	0.6455	0.7550	0.99892
7	0.4364	0.1770	0.1889	0.23163
8	1.4554	1.4796	1.2664	1.29230
9	1.0103	0.4497	0.1524	0.10000
10	2.1382	1.4556	1.4054	2.06910
11	0.8583	1.2238	3.0896	1.11570
12	1.2718	0.2739	1.6398	0.21684
13	3.0807	1.9174	6.1505	2.59770
14	0.2677	0.1170	0.4268	0.10000
15	4.2403	3.5535	3.9541	2.32330
16	2.0098	1.3360	2.0265	1.58000
17	1.5956	0.6289	2.5121	0.10000
18	6.2338	4.8335	3.1521	6.78920
19	2.5793	0.6062	2.4011	0.10000
20	3.0520	5.4393	7.4375	6.67190
21	1.8121	1.8435	1.7242	2.03730
22	1.2986	1.8435	6.1541	0.29086
23	5.8810	8.1759	5.0404	9.83100
24	0.2324	0.3209	0.8897	0.60194
25	7.7536	10.9800	7.7439	10.05500
26	2.6871	2.9489	8.9341	4.13750
27	12.5094	10.5243	9.4718	9.40200
28	29.5704	20.4271	26.8170	17.71800
29	8.2910	19.0983	20.6050	15.40400
Weight (kg)	2559.86	2298.61	3403.22	2262.96
Mean weight (kg)	N/A	N/A	4054.20	2370.90
Standard deviation (kg)	N/A	N/A	435.08	78.94

Tab. 17. Natural frequencies (Hz) evaluated at the optimized designs for the 200-bar planar truss.

Frequency No.	Kaveh and Zolghadr [12]		Present work	
	CSS	CSS-BBBC	BBO	CBBO
1	5.000	5.010	5.000	5.001
2	15.961	12.911	16.212	13.569
3	16.407	15.416	17.987	15.270
4	20.748	17.033	24.947	17.190
5	21.903	21.426	26.301	21.694
6	26.995	21.613	29.881	23.723

5 Concluding remarks

This paper introduces a new optimization algorithm for size and shape optimization of truss structures with natural frequency constraints called the CBBO, which combines the biogeography-based optimization and the Chaos theory. In this approach, the new chaotic migration and mutation operators are proposed to enhance the performance of standard BBO algorithm. Both such migration and the mutation operators can help to keep the diversity of whole population on a higher level to avoid habitat's trapping into local optima.

The performance of the proposed algorithm is evaluated using a set of five well-known truss design examples. In each design example, sensitivity analysis was performed for internal parameters (N_H , c_1 , c_2 and α) of the CBBO algorithm to investigate how the CBBO is affected by these parameters and the best combination of them obtained. The results of the sensitivity analysis demonstrate that, for most design examples, the lowest structural weight is obtained for $c_1 = 1$, $c_2 = 1$ and $\alpha = 0.05$.

The numerical results show the efficiency and capabilities of the CBBO in finding the lightest structural weight. For all design examples, the structural weights obtained by CBBO are relatively lighter weights than those previously reported in the literature (except for Case 1 of first design example). Moreover, it is demonstrated that the standard deviation of optimized weights obtained by the proposed algorithm is less than other methods. It means that CBBO can provide higher quality and more robust designs.

References

- 1 **Grandhi R**, *Structural optimization with frequency constraints - A review*, AIAA Journal, **31**(12), (1993), 2296–2303, DOI 10.2514/3.11928.
- 2 **Grandhi R, Venkayya V**, *Structural optimization with frequency constraints*, AIAA Journal, **26**(7), (1988), 858–866, DOI 10.2514/3.9979.
- 3 **Sedaghati R, Suleman A, Tabarrok B**, *Structural Optimization with Frequency Constraints Using the Finite Element Force Method*, AIAA Journal, **40**(2), (2002), 382–388, DOI 10.2514/2.1657.
- 4 **Sergeyev O, Mróz Z**, *Sensitivity analysis and optimal design of 3D frame structures for stress and frequency constraints*, Computers & Structures, **75**(2), (2000), 167–185, DOI 10.1016/S0045-7949(99)00088-7.
- 5 **Wang D, Zha W, Jiang J**, *Truss Optimization on Shape and Sizing with Frequency Constraints*, AIAA Journal, **42**(3), (2004), 622–630, DOI 10.2514/1.1711.
- 6 **Goldberg D**, *Genetic algorithm in search, optimization and machine learning*, Addison-Wesley, 1989.
- 7 **Kennedy J, Eberhart R**, *Particle swarm optimization*, IEEE international conference on neural networks, In., 1995, pp. 1942–1948.
- 8 **Kaveh A, Talatahari S**, *A novel heuristic optimization method: charged system search*, Acta Mechanica, **213**(3-4), 267–289, DOI 10.1007/s00707-009-0270-4.
- 9 **Erol O, Eksin I**, *A new optimization method: Big Bang–Big Crunch*, Advances in Engineering Software, **37**(2), (2006), 106–111, DOI 10.1016/j.advengsoft.2005.04.005.
- 10 **Lingyun W, Mei Z, Guangming W, Guang M**, *Truss optimization on shape and sizing with frequency constraints based on genetic algorithm*, Computational Mechanics, **35**(5), (2005), 361–368, DOI 10.1007/s00466-004-0623-8.
- 11 **Gomes M**, *Truss optimization with dynamic constraints using a particle swarm algorithm*, Expert Systems and Applications, **38**(1), (2011), 957–968, DOI 10.1016/j.eswa.2010.07.086.
- 12 **Kaveh A, Zolghadr A**, *Democratic PSO for truss layout and size optimization with frequency constraints*, Computers & Structures, **130**, (2014), 10–21, DOI 10.1016/j.compstruc.2013.09.002.
- 13 **Kaveh A, Zolghadr A**, *Truss optimization with natural frequency constraints using a hybridized CSS–BBBC algorithm with trap recognition capability*, Computers & Structures, **102–103**, (2012), 14–27, DOI 10.1016/j.compstruc.2012.03.016.
- 14 **Simon D**, *Biogeography-Based Optimization*, IEEE Transactions on Evolutionary Computation, **12**(6), (2008), 702–713, DOI 10.1109/TEVC.2008.919004.
- 15 **MacArthur R, Wilson E**, *The Theory of Biogeography*, Princeton University Press; USA, 1967.
- 16 **Boussaid I, Chatterjee A, Siarry P, Ahmed-Nacer M**, *Biogeography-based optimization for constrained optimization problems*, Computers & Operations Research, **39**(12), (2012), 3293–3304, DOI 10.1016/j.cor.2012.04.012.
- 17 **Simon D, Rarick R, Ergezer M, Du D**, *Analytical and numerical comparisons of biogeography-based optimization and genetic algorithms*, Information Sciences, **181**(7), (2011), 1224–1248, DOI 10.1016/j.ins.2010.12.006.
- 18 **Singh U, Kumar H, Kamal T**, *Design of Yagi-Uda Antenna Using Biogeography Based Optimization*, IEEE Transactions on Antennas and Propagation, **58**(10), (2010), 3375–3379, DOI 10.1109/TAP.2010.2055778.
- 19 **Bhattacharya A, Chattopadhyay P**, *Biogeography-Based Optimization for Different Economic Load Dispatch Problems*, IEEE Transactions on Power Systems, **25**(2), (2010), 1064–1077, DOI 10.1109/TPWRS.2009.2034525.
- 20 **Liu B, Wang L, Jin Y, Tang F, Huang D**, *Improved particle swarm optimization combined with chaos*, Chaos, Solitons & Fractals, **25**(5), (2005), 1261–1271, DOI 10.1016/j.chaos.2004.11.095.
- 21 **Coelho L, Mariani V**, *Use of chaotic sequences in a biologically inspired algorithm for engineering design optimization*, Expert Systems with Applications, **34**(3), (2008), 1905–1913, DOI 10.1016/j.eswa.2007.02.002.
- 22 **Gao W, Liu S, Huang L**, *Particle swarm optimization with chaotic opposition-based population initialization and stochastic search technique*, Communications in Nonlinear Science and Numerical Simulation, **17**(11), (2012), 4316–4327, DOI 10.1016/j.cnsns.2012.03.015.
- 23 **Gandomi A, Yun G, Yang X, Talatahari S**, *Chaos-enhanced accelerated particle swarm optimization*, Communications in Nonlinear Science and Numerical Simulation, **18**(2), (2013), 327–340, DOI 10.1016/j.cnsns.2012.07.017.
- 24 **He Y, Zhou J, Lu N, Qin H, Lu Y**, *Differential evolution algorithm combined with chaotic pattern search*, Kybernetika, **46**(4), (2010), 684–696.
- 25 **Alatas B**, *Chaotic harmony search algorithms*, Applied Mathematics and Computation, **216**(9), (2010), 2687–2699, DOI 10.1016/j.amc.2010.03.114.
- 26 **dos Santos Coelho L, Herrera B**, *Fuzzy Identification Based on a Chaotic Particle Swarm Optimization Approach Applied to a Nonlinear Yo-yo Motion System*, IEEE Transactions on Industrial Electronics, **54**(6), (2007), 3234–3245, DOI 10.1109/TIE.2007.896500.
- 27 **May R**, *Simple mathematical models with very complicated dynamics*, Nature, **261**(459-467), (1976).
- 28 **Parlitz U, Ergezing S**, *Robust communication based on chaotic spreading sequences*, Physics Letters A, **188**(2), (1994), 146–150, DOI 10.1016/0375-9601(84)90009-4.
- 29 **Kaveh A, Zolghadr A**, *Shape and size optimization of truss structures with frequency constraints using enhanced charged system search algorithm*, Asian Journal of Civil Engineering, **12**, (2011), 487–509.
- 30 **Kaveh A, Mahdavi V**, *Optimal design of structures with multiple natural frequency constraints using a hybridized BB-BC/Quasi-Newton algorithm*, Periodica Polytechnica Civil Engineering, **57**(1), (2013), 27–38, DOI 10.3311/PPci.2139.

- 31 **Kaveh A, Javadi S**, *An efficient hybrid particle swarm strategy, ray optimizer, and harmony search algorithm for optimal design of truss structures*, *Periodica Polytechnica Civil Engineering*, **58**(2), (2014), 155–171, DOI 10.3311/PPci.7550.
- 32 **Kaveh A, Javadi S**, *Shape and size optimization of trusses with multiple frequency constraints using harmony search and ray optimizer for enhancing the particle swarm optimization algorithm*, *Acta Mechanica*, **225**(6), (2014), 1595–1605, DOI 10.1007/s00707-013-1006-z.
- 33 **Kaveh A, Zolghadr A**, *Comparison of nine meta-heuristic algorithms for optimal design of truss structures with frequency constraints*, *Advances in Engineering Software*, **76**, (2014), 9–30, DOI 10.1016/j.advengsoft.2014.05.012.
- 34 **Lin J, Chen W, Yu Y**, *Structural optimization on geometrical configuration and element sizing with statical and dynamical constraints*, *Computers & Structures*, **15**(5), (1982), 507–515, DOI 10.1016/0045-7949(82)90002-5.